Experimental study of $\Delta I = 1$ bands in ^{111}In

P. Banerjee,[1] S. Ganguly,[2] M. K. Pradhan,[1] H. P. Sharma,[3] S. Muralithar,[4] R. P. Singh,[4] and R. K. Bhowmik[4]

[1]*Saha Institute of Nuclear Physics, Sector 1, Block AF, Bidhan Nagar, Kolkata 700 064, India*

[2]*Department of Physics, Chandernagore College, Chandernagore, Hooghly 712136, India*

[3]*Benaras Hindu University, Varanasi 221005, India*

[4]*Inter University Accelerator Centre, New Delhi 110067, India*

(Received 4 December 2010; published 28 February 2011)

The two $\Delta I = 1$ bands in ^{111}In, built upon the 3461.0 and 4931.8 keV states, have been studied. The bands were populated in the reaction ^{100}Mo(^{19}F, $\alpha 4n\gamma$) at a beam energy of 105 MeV. Mean lifetimes of nine states, four in the first and five in the second band, have been determined for the first time from Doppler shift attenuation data. The deduced $B(M1)$ rates and their behavior as a function of level spin support the interpretation of these bands within the framework of the shears mechanism. The geometrical model of Machiavelli *et al.* has been used to derive the effective gyromagnetic ratios for the two bands.

DOI: 10.1103/PhysRevC.83.024316 PACS number(s): 21.10.Re, 21.10.Tg, 25.70.Gh, 27.60.+j

I. INTRODUCTION

Nuclei in the $A = 110$ mass region contain rich structural information. Although, these nuclei, with the proton number close to the $Z = 50$ shell closure, are normally expected to be spherical, collective states arising from proton excitations across the shell gap have been reported. The two-particle–two-hole (2p-2h) proton excitations in ^{108}Sn, ^{109}Sb, and ^{110}Te, resulting in $\Delta I = 2$ decoupled bands, have been reported in the literature to have considerable deformation [1,2]. These intruder-type rotational bands have been shown to terminate smoothly in a noncollective oblate state ($\gamma = 60^\circ$) at a high spin when all the valence particles have aligned along the "rotation" axis. A similar decoupled terminating sequence has also been identified recently in ^{111}Sn by the present group [3]. In addition, long sequences of transitions forming strongly coupled bands have been found in ^{110,112}Te. They are interpreted in terms of deformed structures built on proton 1p-1h excitations that reach termination around a spin of $40\hbar$ [4].

The other interesting feature for nuclei near $A = 110$ is the observation of weakly deformed $\Delta I = 1$ bands consisting of intense dipole transitions that involve the perpendicular coupling of hole(s) in high-Ω, $g_{9/2}$ proton orbital with neutrons in low-Ω, $h_{11/2}$ shell. The $B(M1)$ rates for these bands drop off rapidly as a function of rotational frequency, which is a consequence of the shears dynamics. Such bands have been identified in ^{105}Sn and ^{108}Sb mainly from theoretical considerations using the tilted axis cranking (TAC) calculations and in ^{106,108}Sn using the experimental $B(M1)$ rates [5–7]. The experimental data for nuclei with $Z < 50$ is however, inconclusive. Although dipole bands have previously been observed in ^{110}Cd and ^{111,113}In [8–10], an unambiguous interpretation of the structures of the states belonging to these bands is not reported. Several weakly deformed bands have been observed in these nuclei based on at most a 1p-1h proton excitation. In ^{111}In, three such strongly coupled sequences (bands 6, 8, and 10 in Ref. [9]), with a large K value, have been reported. These bands, observed up to modest spins, drop off quickly in $B(M1)/B(E2)$ strength, but the absence (or a very weak nature) of the crossover $E2$ transitions in most cases prevents a definite inference. It is of interest therefore to look into these bands in ^{111}In further from a direct study of the $B(M1)$ rates of the transitions in order to understand if the shears mechanism is indeed responsible for the structure of the states.

II. EXPERIMENTAL DETAILS AND RESULTS

Excited states of ^{111}In were populated in the ^{100}Mo(^{19}F, $\alpha 4n\gamma$) reaction at a beam energy of 105 MeV at the 15UD Pelletron accelerator at the Inter University Accelerator Centre (IUAC), New Delhi. The target consisted of isotopically enriched (99.5%) ^{100}Mo with a thickness of 2 mg/cm^2 evaporated on a 8 mg/cm^2 gold foil. About 25×10^9 twofold and higher γ-γ coincidence events were collected using the Indian National Gamma Array (INGA) comprising 15 Compton-suppressed clover detectors. Four of these detectors were placed at 90° and 148°, three at 32°, and two each at 57° and 123° to the beam direction.

Gated energy spectra with a dispersion of 0.5 keV per channel were generated from several 4096 × 4096 matrices, obtained from sorting the raw data of the appropriate detectors. The spectra for lifetime analysis using the Doppler shift attenuation (DSA) technique, for example, were obtained from matrices formed from coincidences between either the forward (32°) or the backward (148°) angle events with those in the remaining detectors. The data were analyzed using the computer code INGASORT [11].

The directional correlation (DCO) of γ-rays deexciting oriented states was obtained as described in [12]. The DCO ratios ($R_{\rm DCO}$), defined as

$$R_{\rm DCO} = \frac{I_\gamma \text{ at } 148^\circ \text{ gated by } \gamma_G \text{ at } 90^\circ}{I_\gamma \text{ at } 90^\circ \text{ gated by } \gamma_G \text{ at } 148^\circ},$$

with I_γ being the intensity of the γ-ray of interest in coincidence with γ_G, were compared with the theoretical DCO ratios for assignment of spin I and the γ-ray multipole mixing ratios δ. A width of $\sigma = 0.3I$ was used for the

presumed Gaussian distribution of the magnetic substate population. Gates were set mostly on $E2$ transitions. For some of the γ-rays, however, strong $\Delta I = 1$ transitions with known δ values were used as gates. Other relevant details of the $R_{\rm DCO}$ measurements are stated in Ref. [12].

Level lifetimes τ were estimated from the DSA data at both forward (32°) and backward (148°) angles using the computer code LINESHAPE [13]. The details of the slowing down history of the recoils (moving with an initial recoil velocity $\beta = 0.0174$) in the target and backing were simulated using a Monte Carlo technique, as described in Ref. [3]. The shell-corrected stopping powers of Northcliffe-Schilling [14] were used. Corrections due to feedings from discrete higher energy states and the continuum were incorporated in the lifetime results [3]. For this, the side-feeding times were assumed to be 0.1 ps for the highest observed state in each band and followed the general trend that they increased progressively for the lower-lying states. This procedure is found to reproduce the reported lifetime results [3] of the 2p-2h band in ^{111}Sn, also populated in the present experiment. Side-feeding intensities were estimated from the γ-ray relative intensities determined from the gated data at 57° and 123° to the beam direction. Errors in the level lifetimes include the effect of a 50% uncertainty in the side-feeding times and the statistical uncertainties in the data.

Figure 1 shows the partial level scheme of ^{111}In based on the present experimental results. Although several bands were populated in the experiment, only the two bands, marked band 1 and band 2, are shown in the figure. It also shows the interband transitions and other transitions that connect these two bands with other bands. All states shown in Fig. 1 have been reported previously [9]. However, the present data could not confirm the previously reported weak 764 keV γ-ray depopulating the 8680.5 keV $(43/2^+)$ state (see band 2 in Fig. 1). The γ-ray relative intensities were determined from gated data at 57° and 123° to the beam direction. Relative intensities for the inband transitions are given in Table I along with the results of the $R_{\rm DCO}$ measurements. Table II summarizes the lifetime results and the reduced transition probabilities $B(M1)$ and $B(E2)$. Relative intensities of other transitions (not given in Table I) are indicated by the widths of the transitions in Fig. 1. The γ-ray branching ratios (see Table II) for band 1 are in agreement within experimental errors with those adopted in the literature [15].

The present $R_{\rm DCO}$ results, summarized in Table I, permit unambiguous spin assignments for all states belonging to band 1 and for states up to 6538.1 keV in band 2. The earlier spin assignments for 5878.0 and 6538.1 keV were tentative [9]. Gamma-ray multipole mixing ratios δ, reported here for the first time for these bands, indicate that the $\Delta I = 1$ transitions are predominantly $M1$ in nature with small $E2$ admixtures. Three crossover $E2$ transitions are observed in band 1 but none in the other band.

Lifetime results are not reported in the literature for the two bands in ^{111}In. Lifetimes of four states in band 1 and five states in band 2 have been determined from the DSA data in the present work. Besides, an upper limit of the lifetime has been estimated for the $(41/2^+)$ 7916.5 keV state in band 2.

Gated spectra with gates set on lower-lying transitions are used for both bands. Representative gated spectra for the 371.3 and 534.8 keV transitions (at 90° and 148° with respect to the beam), deexciting the 4283.5 and 5331.7 keV states in band 1, and for 373.0 and 487.0 keV transitions (at 90° and 32° with respect to the beam), depopulating the 6051.1 and 6538.1 keV states in band 2, respectively, are shown in Fig. 2. The contribution of the 371.3 keV γ-ray in the spectrum for the 373.0 keV transition (and vice versa) are accounted for in the analyses.

Mean lifetimes of $0.66^{+0.21}_{-0.14}$, $0.30^{+0.10}_{-0.07}$, $0.65^{+0.23}_{-0.16}$, and $0.73^{+0.25}_{-0.16}$ ps have been determined for the 4283.5, 4796.9, 5331.7, and 5878.0 keV states, respectively, belonging to band 1. For band 2, lifetime values of $1.60^{+0.25}_{-0.17}$, $0.54^{+0.07}_{-0.05}$, $0.38^{+0.09}_{-0.07}$, $0.30^{+0.07}_{-0.05}$, and 0.28 ± 0.07 ps were estimated for the 5398.8, 5678.1, 6051.1, 6538.1, and 7175.0 keV states, respectively. An upper limit of mean life of 0.20 ps has been estimated for the highest observed state at 7916.5 keV in this band. Errors in the lifetime results were assigned as discussed above.

The $B(M1)$ rates determined from the present lifetime results, δ values, and γ-ray branchings (see Table II) are seen to be large compared to those found for $M1$ transitions in normal deformed bands. The $B(M1)$ values deduced from these lifetime results decrease with spin for both bands. In band 1, the B$(M1)$ value decreases from $1.62^{+0.43}_{-0.40}$ $\mu_N{}^2$ for the 371.3 keV, $27/2^+ \rightarrow 25/2^+$ transition to 0.35 ± 0.10 $\mu_N{}^2$ for the 546.3 keV, $33/2^+ \rightarrow 31/2^+$ transition. Weak crossover $E2$ transitions are observed from the three highest energy states in this band. The corresponding $B(E2)$ rates show that the deformations are small with an average value of $\beta_2 \sim 0.05$.

No crossover $E2$ transitions are observed in band 2. The states decay by transitions that are almost pure dipole in nature as in band 1 (see Table I). However, the $B(M1)$ rates are comparatively larger. The 279.3 keV transition from the 5678.1 keV level has the largest $B(M1)$ value of $4.64^{+0.47}_{-0.53}$ $\mu_N{}^2$. While transitions deexciting higher energy states have progressively smaller B$(M1)$ rates as for band 1, the 232.1 keV γ-ray from the lower-lying 5398.8 keV state has a smaller $B(M1)$ value relative to that for the 279.3 keV transition (Table II). A measurement of the mean life for the lowest 234.9 keV transition, rendered impossible due to the small Doppler shift observed for the γ-ray in this work, would be interesting in this context.

III. DISCUSSION

As already stated, the states belonging to bands 1 and 2 in ^{111}In decay by transitions that are predominantly dipole in nature. Weak crossover $E2$ transitions are observed in band 1 only, and the corresponding quadrupole deformations are small. Besides, both bands are found to extend only over a short range of angular momenta. These observations suggest that the bands are based on configurations that do not involve a proton excitation from the $g_{9/2}$ orbital. Band 1 can therefore be associated with the probable configuration $\pi(g_{9/2}^{-1}) \otimes \nu(h_{11/2}^2)$, and band 2 with an aligned $g_{7/2}$ neutron pair coupled to it, as suggested by Vaska *et al.* [9] based on a comparison of

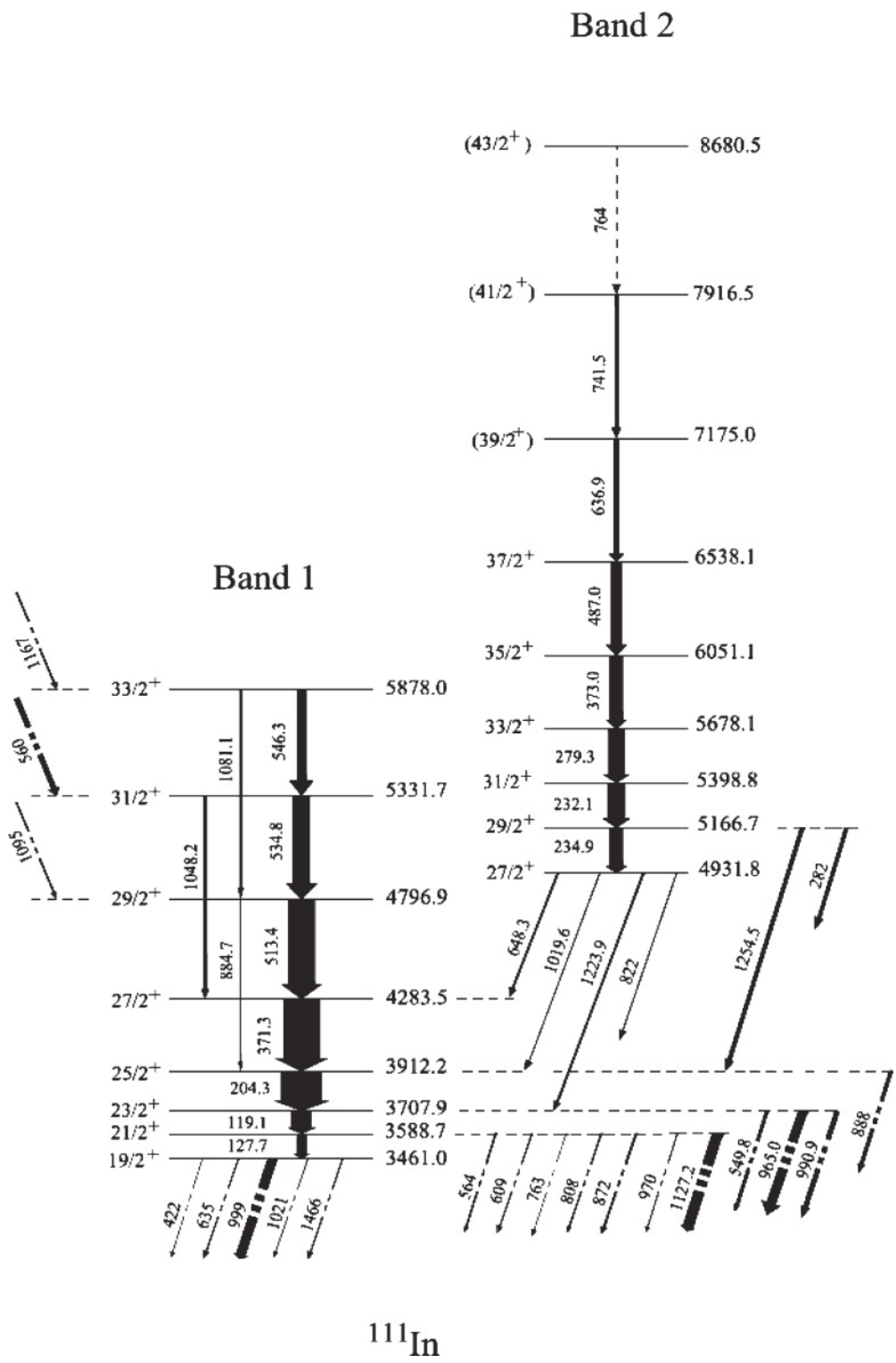

FIG. 1. Partial Level scheme of ^{111}In obtained in the present work. The γ-ray relative intensities are indicated by the widths of the transitions. (see text)

the bandhead spins and aligned angular momenta for the two bands in ^{111}In with similar bands in ^{110}Cd [16].

These valence configurations involving a high-j proton hole and neutron particles favor the interpretation of these two bands within the framework of the shears mechanism. The tilted-axis-cranking (TAC) model of Frauendorf *et al.* [17] has explained similar bands in the Pb region as arising from the coupling of two long j vectors ($\vec{j}_\pi$ and $\vec{j}_\nu$) such that the total angular momentum is generated by a gradual alignment of the proton and neutron spin vectors in a way that resembles the

TABLE I. Level and γ-ray energies, γ-ray relative intensities (RI), DCO ratios, multipole mixing ratios, and spin assignments for levels in bands 1 and 2 in ^{111}In.

E_x (keV)	E_γ (keV)	RI	$R_{\rm DCO}$	Gate (keV)	Multipole mixing ratio	$I_i^\pi \rightarrow I_f^\pi$
Band 1						
3588.7	127.7	9.3 ± 0.9	–	–	–	$21/2^+ \rightarrow 19/2^+$[a]
3707.9	119.1	18.2 ± 1.0	–	–	–	$23/2^+ \rightarrow 21/2^+$[a]
3912.2	204.3	37.1 ± 1.6	0.76 ± 0.05	1001[b]	$0.16^{+0.06}_{-0.10}$	$25/2^+ \rightarrow 23/2^+$
4283.5	371.3	33.3 ± 2.5	1.38 ± 0.26	1001[b]	0.20 ± 0.11	$27/2^+ \rightarrow 25/2^+$
4796.7	513.4	24.4 ± 2.9	0.49 ± 0.06	1401[c]	$-0.04^{+0.04}_{-0.08}$	$29/2^+ \rightarrow 27/2^+$
	884.7	1.0 ± 0.3	–	–	–	$29/2^+ \rightarrow 25/2^+$
5331.7	534.8	15.8 ± 1.5	0.98 ± 0.11	371.3	$0.18^{+0.13}_{-0.12}$	$31/2^+ \rightarrow 29/2^+$
	1048.2	2.3 ± 0.7	–	–	–	$31/2^+ \rightarrow 27/2^+$
5878.0	546.3	8.6 ± 1.5	1.07 ± 0.12	371.3	$0.25^{+0.14}_{-0.15}$	$33/2^+ \rightarrow 31/2^+$
	1081.1	2.4 ± 0.7	–	–	–	$33/2^+ \rightarrow 29/2^+$
Band 2						
5166.7	234.9	12.1 ± 1.0	0.60 ± 0.08	1401[c]	$0.05^{+0.05}_{-0.08}$	$29/2^+ \rightarrow 27/2^+$
5398.8	232.1	15.6 ± 1.3	0.75 ± 0.07	1401[c]	$0.17^{+0.07}_{-0.05}$	$31/2^+ \rightarrow 29/2^+$
5678.1	279.3	14.8 ± 1.4	0.81 ± 0.11	1401[c]	$0.20^{+0.10}_{-0.07}$	$33/2^+ \rightarrow 31/2^+$
6051.1	373.0	11.9 ± 3.2	–	–	–	$35/2^+ \rightarrow 33/2^+$[a]
6538.1	487.0	9.8 ± 3.7	0.64 ± 0.19	1401[c]	$0.07^{+0.15}_{-0.18}$	$37/2^+ \rightarrow 35/2^+$
7175.0	636.9	5.0 ± 2.0	–	–	–	$(39/2^+) \rightarrow 37/2^+$
7916.5	741.5	3.2 ± 1.7	–	–	–	$(41/2^+) \rightarrow (39/2^+)$
8680.5	764	–	–	–	–	$(43/2^+) \rightarrow (41/2^+)$

[a]Spin assignment from Ref. [9].
[b]$15/2^- \rightarrow 13/2^+$, $E1$ transition from Ref. [9].
[c]$13/2^+ \rightarrow 9/2^+$, $E2$ transition from Ref. [9].

closing of a pair of shears. Such bands are therefore referred to as "shears bands." Indeed, the large $B(M1)$ rates at low spins and their decline with increasing spin, as reported for several nuclei in the Pb region and observed in the present work (see Table II) for the two bands in ^{111}In, constitute the most conclusive experimental fingerprint for this interpretation. While the $B(M1)$ values for the inband transitions decrease continually up to the highest observed state in both bands, the experimental

TABLE II. Present experimental results on mean lifetime τ and reduced transition probabilities $B(M1)$ and $B(E2)$ for the $\Delta I = 1$ bands in ^{111}In.

E_x (keV)	E_γ (keV)	Spin $J_i^\pi \rightarrow J_f^\pi$	Branching ratio (%)	Multipole mixing ratio (δ)	τ (ps)	$B(M1)$ ($\mu_N{}^2$)	$B(E2)$ (W.u.)
Band 1							
4283.5	371.3	$27/2^+ \rightarrow 25/2^+$	100	0.20 ± 0.10	$0.66^{+0.21}_{-0.14}$	$1.62^{+0.43}_{-0.40}$	
4796.9	513.4	$29/2^+ \rightarrow 27/2^+$	96 ± 11	$-0.04^{+0.04}_{-0.08}$	$0.30^{+0.10}_{-0.07}$	$1.30^{+0.50}_{-0.30}$	
	884.7	$29/2^+ \rightarrow 25/2^+$	4 ± 1.3	$E2$			$6.4^{+1.9}_{-1.6}$
5331.7	534.8	$31/2^+ \rightarrow 29/2^+$	87.4 ± 11.7	$0.18^{+0.08}_{-0.07}$	$0.65^{+0.23}_{-0.16}$	$0.50^{+0.16}_{-0.13}$	
	1048.2	$31/2^+ \rightarrow 27/2^+$	12.6 ± 4.0	$E2$			$4.0^{+1.3}_{-1.0}$
5878.0	546.3	$33/2^+ \rightarrow 31/2^+$	78.4 ± 19.3	$0.25^{+0.08}_{-0.09}$	$0.73^{+0.25}_{-0.16}$	0.35 ± 0.10	
	1081.1	$33/2^+ \rightarrow 29/2^+$	21.6 ± 7.7	$E2$			$5.2^{+1.5}_{-1.3}$
Band 2							
5398.8	232.1	$31/2^+ \rightarrow 29/2^+$	100	$0.17^{+0.07}_{-0.05}$	$1.60^{+0.25}_{-0.17}$	$2.74^{+0.32}_{-0.37}$	
5678.1	279.3	$33/2^+ \rightarrow 31/2^+$	100	$0.20^{+0.10}_{-0.07}$	$0.54^{+0.07}_{-0.05}$	$4.64^{+0.47}_{-0.53}$	
6051.1	373.0	$35/2^+ \rightarrow 33/2^+$	100	0.25 ± 0.20	$0.38^{+0.09}_{-0.07}$	$2.71^{+0.61}_{-0.52}$	
6538.1	487.0	$37/2^+ \rightarrow 35/2^+$	100	$0.07^{+0.15}_{-0.18}$	$0.30^{+0.07}_{-0.05}$	$1.63^{+0.33}_{-0.31}$	
7175.0	636.9	$(39/2^+) \rightarrow 37/2^+$	100	–	0.28 ± 0.07	$0.79^{+0.26}_{-0.16}$	
7916.5	741.5	$(41/2^+) \rightarrow (39/2^+)$	100	–	<0.20	>0.70	

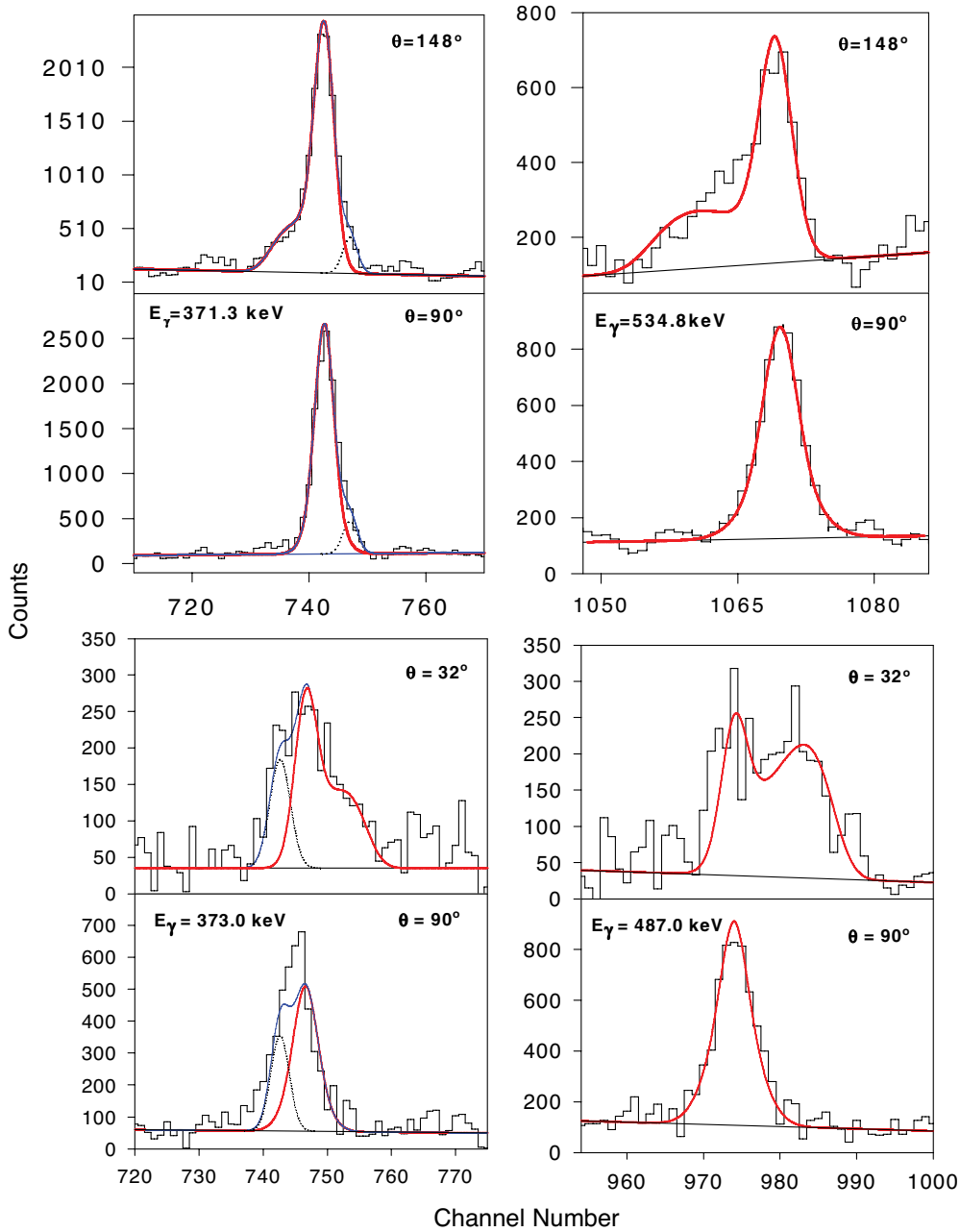

FIG. 2. (Color online) Experimental data and line-shape fits (continuous line) for the 371.3 and 534.8 keV γ-rays in band 1 (upper panels) and 373.0 and 487.0 keV γ-rays in band 2 (lower panels) in ^{111}In. The spectra are labeled by the angles at which the detectors were placed. The dashed lines indicate the contributions of 373.0 keV line to the line shape for 371.3 keV transition and that of the 371.3 keV line to the line shape for 373.0 keV.

$B(M1)/B(E2)$ ratios for the γ-rays in band 1 also decrease from 64.1 ± 26.7 $(\mu_N/e\text{b})^2$ for the $29/2^+$ state to 21.2 ± 8.3 $(\mu_N/e\text{b})^2$ for the $33/2^+$ state. Furthermore, the $B(E2)$ rates for transitions in band 1 also show a decreasing trend as the shears close (see Table II). In the absence of collective rotation, the $B(E2)$ values should become zero, since the charge distribution is symmetric around the rotation axis.

The validity of the shears mechanism as a mode of generating angular momentum has been previously tested using the semiclassical model of Macchiavelli *et al.* [18]. The shears angle θ in this model (which is the angle between j_π and j_ν, the proton and neutron spin vectors, respectively,) for a given state I is given by

$$\cos\theta = \frac{I_{\text{sh}}(I_{\text{sh}}+1) - j_\nu(j_\nu+1) - j_\pi(j_\pi+1)}{2[j_\nu(j_\nu+1)j_\pi(j_\pi+1)]^{1/2}}, \qquad (1)$$

with $\vec{j}_\pi + \vec{j}_\nu = \vec{I}$, and I_{sh} is the shears contribution to the I.

The $B(M1)$ values, which are proportional to the square of the perpendicular (to the spin vector $\vec{I}$) component of the

TABLE III. Calculated values of spin contribution from shears I_{sh}, shears angle θ, and proton angle θ_π for states belonging to bands 1 and 2.

Level spin I ($\hbar$)	I_{sh} ($\hbar$)	Shears angle θ (deg)	Proton angle θ_π (deg)
Band 1 ($j_\pi = 4.5\hbar$, $j_\nu = 8\hbar$)			
9.5	9.5	88.0	59.1
10.5	9.9	82.0	54.7
11.5	10.4	75.6	50.1
12.5	10.8	68.9	45.3
13.5	11.2	61.6	40.3
14.5	11.6	53.3	34.7
15.5	12.1	43.7	28.3
16.5	12.5	31.5	20.3
Band 2 ($j_\pi = 4.5\hbar$, $j_\nu = 12\hbar$)			
13.5	13.5	83.1	63.5
14.5	14.5	69.3	52.1
15.5	15.5	52.9	39.2
16.5	16.5	29.7	21.7
Band 2 ($j_\pi = 4.5\hbar$, $j_\nu = 15\hbar$)			
16.5	16.5	81.0	65.2
17.5	17.1	73.1	58.3
18.5	17.7	64.6	51.1
19.5	18.3	55.0	43.2
20.5	18.9	43.7	34.1
21.5	19.5	28.9	22.3

magnetic moment μ is given by

$$B(M1, I \rightarrow I-1) = \frac{3}{8\pi}\mu_\perp^2 = \frac{3}{8\pi} g_{\rm eff}^2 j_\pi^2 \sin^2\theta_\pi [\mu_N{}^2], \qquad (2)$$

where $g_{\rm eff} = g_\pi - g_\nu$ and $\tan\theta_\pi = j_\nu \sin\theta/(j_\pi + j_\nu \cos\theta)$, θ_π being the angle between j_π and I. Other details of the model are given in Ref. [18].

This model has been applied in the present work in order to get a clear insight into the structures of bands 1 and 2. Assuming a perpendicular coupling of the spin vectors at the bandhead and $j_\pi = 4.5\,\hbar$ for both bands (corresponding to the proton configuration adopted above), neutron spins of $j_\nu = 8\,\hbar$ and $12\hbar$ are determined [using Eq. (1)] for bands 1 and 2, respectively, that reproduce the respective bandhead spin. These j_π and j_ν values are then used to calculate the shears angle θ (and hence θ_π) for the higher spin states. The results are summarized in Table III. As noted above, these calculations use I_{sh} which are estimated using the method outlined in Refs. [19,20]. The core component $I_{\rm core}$ is assumed to be a linear function of spin, i.e., $I_{\rm core} = (\Delta R/\Delta I)(I - I_b)$. Here ΔR is the difference between the spin of the highest observed state ($I_{\rm max}$) and the maximum spin that can be generated from the fully closed blades of the shears (i.e., $j_\pi + j_\nu$), and ΔI is the range of angular momenta over which the band is observed (i.e., $I_{\rm max} - I_{\rm bandhead}$).

As seen from Table III, the states belonging to band 1 have a somewhat large core contribution, with a maximum of 24% for the $33/2^+$ highest observed state. It is plausible that the crossover $E2$ transitions observed in this band and the somewhat large $B(E2) = 5.2^{+1.5}_{-1.3}$ W.u. for the $33/2^+ \rightarrow 29/2^+$ transition arise due to the presence of this significant collective component.

In band 2, the proton and neutron spin vectors $j_\pi = 4.5\hbar$ and $j_\nu = 12\hbar$, respectively, couple to form a maximum angular momentum of $I_{\rm max} = 16.5\hbar$, although the band extends up to $41/2^+$ (tentatively up to $43/2^+$). Evidently, states with spin larger than $I_{\rm max}$ can be formed only with an additional pair of aligned particles, ostensibly neutrons in this case in the normal parity $(d_{5/2}, g_{7/2})$ orbitals (see Ref. [21]). Experimentally, this alignment is observed at a rotational frequency $\hbar\omega = 0.33$ MeV/$\hbar$, corresponding to a level spin of $33/2^+$ [21]. Furthermore, the relatively large $B(M1)$ value for the 279.3 keV transition from the $33/2^+$ state compared to that for the 232.1 keV γ-ray from the $31/2^+$ state is a possible consequence of this alignment in the light of the shears mechanism. Taking the $33/2^+$ state as the bandhead for the aligned sequence, a perpendicular coupling of the spin vectors yields $j_\nu = 15\hbar$ (with $j_\pi = 4.5\hbar$). These spin vectors can then couple to $I_{\rm max} = 19.5\hbar$. With the highest observed state in this sequence having a spin of $41/2^+$, it is apparent that core contribution is indeed small (7.8% for the $41/2^+$ state) for the states of band 2, consistent with the absence of crossover $E2$ transitions.

Figure 3 shows a plot of the experimental $B(M1)$ values as a function of the shears angle θ for band 1 and and for the aligned configuration in band 2. The continuous lines show the best fits of Eq. (2) to the experimental $B(M1)$ results leading to effective gyromagnetic ratios of $g_{\rm eff} = 1.23$ and 1.27 for band 1 and the aligned configuration in band 2, respectively. These $g_{\rm eff}$ results are in fair agreement with values expected for nuclei in this mass region obtained using the single-particle

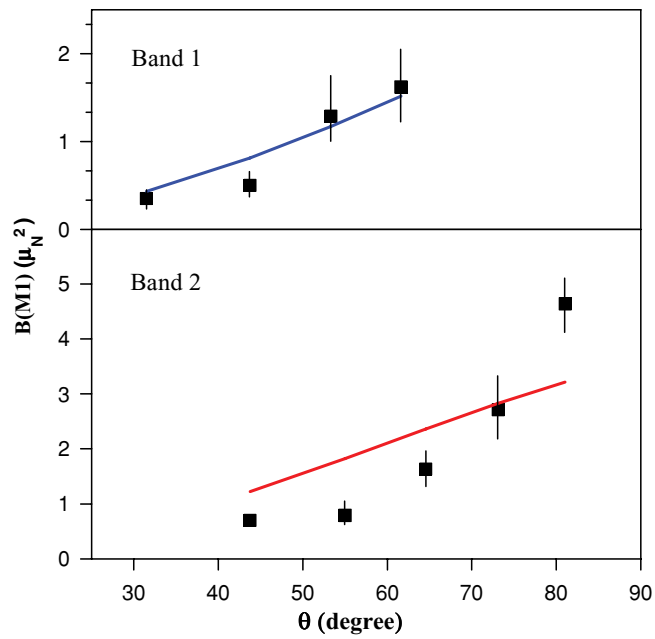

FIG. 3. (Color online) Experimental $B(M1)$ values as a function of shears angle θ for band 1 (upper panel) and band 2 (lower panel). The continuous lines represent the fits of Eq. (2) to the experimental $B(M1)$ values using the semiclassical model of Macchiavelli *et al.* [18].

g factors for the orbitals involved in the configurations of the two bands [22].

Since the core contribution is small for the states belonging to band 2, the residual interaction strength between the proton (hole) and neutron (particle) blades can be derived using the prescription of Macchiavelli *et al.* [18]. For a proton and neutron interacting via a term of the form $V_2 P_2(\cos\theta)$, the interaction is represented by

$$V_{\pi\nu}(\theta) = V_o + V_2 P_2(\theta). \quad (3)$$

Fits of this expression to the experimental level energies for band 2 yield $V_2 \sim 1.0$ and $\sim$2.5 MeV before and after the alignment, respectively. The increase in the effective particle-hole interaction strength is consistent with the availability of an additional neutron pair as a constituent of the neutron blade following the alignment.

ACKNOWLEDGMENTS

The authors thank Dr. Amit Roy, Inter University Accelerator Centre (IUAC), New Delhi, for providing the necessary facilities for the work. They acknowledge the assistance of the operating staff of the Pelletron at the IUAC during the experiment. They also thank Mr. Iqbal and the other personnel at the Target Laboratory in the Variable Energy Cyclotron Centre, Kolkata, who helped in the preparation of the targets. One of the authors (S.G.) acknowledges with thanks the financial support provided by the UGC-DAE-CSR vide project number UGC-DAE-CSR-KC/CRS/2009/NP05/1353.

[1] R. Wadsworth *et al.*, Phys. Rev. Lett. **80**, 1174 (1998).
[2] E. S. Paul *et al.*, Phys. Rev. C **76**, 034323 (2007).
[3] S. Ganguly *et al.*, Phys. Rev. C **78**, 037301 (2008).
[4] A. O. Evans *et al.*, Phys. Lett. B **636**, 25 (2006).
[5] A. Gadea *et al.*, Phys. Rev. C **55**, R1 (1997).
[6] D. G. Jenkins *et al.*, Phys. Rev. C **58**, 2703 (1998).
[7] D. G. Jenkins *et al.*, Phys. Lett. B **428**, 23 (1998).
[8] S. Juutinen *et al.*, Nucl. Phys. A **573**, 306 (1994).
[9] P. Vaska *et al.*, Phys. Rev. C **57**, 1634 (1998).
[10] R. S. Chakrawarthy *et al.*, Phys. Rev. C **55**, 155 (1997).
[11] R. K. Bhowmik, INGASORT manual (private communication).
[12] S. Ganguly *et al.*, Nucl. Phys. A **768**, 43 (2006).
[13] J. C. Wells and N. Johnson, Rep. ORNL-6689, 44, 1991 (unpublished).
[14] L. C. Northcliffe and R. F. Schilling, Nucl. Data Tables **7**, (1970).
[15] Jean Blachot, Nucl. Data Sheets **110**, 1239 (2009).
[16] J. Kumpulainen *et al.*, Phys. Rev. C **45**, 640 (1992).
[17] S. Fauendorf, Nucl. Phys. A **557**, 259c (1993).
[18] A. O. Macchiavelli *et al.*, Phys. Rev. C **57**, R1073 (1998).
[19] A. O. Macchiavelli *et al.*, Phys. Rev. C **58**, R621 (1998).
[20] C. J. Chiara *et al.*, Phys. Rev. C **61**, 034318 (2000).
[21] S. Frauendorf and J. Reif, Nucl. Phys. A **621**, 736 (1997).
[22] T. Lonnroth *et al.*, Z. Phys. A **317**, 215 (1984).